Fall 12-18-2015

Computation of a Virtual Tide Corrector to Support Vertical Adjustment of Autonomous Underwater Vehicle Multibeam Sonar Data

Lawrence H. Haselmaier
University of New Orleans, hasel001@gmail.com

Computation of a Virtual Tide Corrector to Support Vertical Adjustment of Autonomous Underwater Vehicle Multibeam Sonar Data

A Thesis

Submitted to the Graduate Faculty of the
University of New Orleans
in partial fulfillment of the
requirements for the degree of

Master of Science
in
Applied Physics

by

Lawrence H. Haselmaier

B.S. The University of Alabama, 2008

December, 2015

The views expressed in this article are those of the author and do not necessarily reflect the official policy or position of the Department of the Navy, Department of Defense, nor the U.S. Government.

For Sarah and Lucy,
Who are with me through the rise and fall,
Keeping me grounded,
And helping me reach the zenith.

Acknowledgment

I want to thank the people and organizations that contributed to this effort. Val Schmidt, Dr. Art Trembanis, Steve Brodet, and Shannon Byrne offered valuable insight into the concepts. Matthew Thompson, Doug Cronin, Wade Ladner, and Michael Bendzlowicz provided expert technical assistance. Dr. Jessica Lovering, Giovanni Morris, Veronica Ladner, Natalie Lamberton, and Anna Manning supplied constructive stylistic advice. My thesis committee, Dr. George Ioup, Dr. Kevin Stokes, and Wade Ladner, gave me guidance and direction throughout the process. Finally, The University of Delaware, The University of New Hampshire, the Canadian Hydrographic Service, and the Naval Oceanographic Office endowed support without which this project would not have been possible.

Table of Contents

List of Figures

List of Tables

List of Acronyms

AUV	Autonomous Underwater Vehicle
EH	Ellipsoid Height
SOP	Standard Operating Procedures
GNSS	Global Navigation Satellite System
SEP	Ellipsoid to Chart Datum Separation
ASV	Autonomous Surface Vehicle
NAVOCEANO	Naval Oceanographic Office
VTC	Virtual Tide Corrector
IHO	International Hydrographic Organization
TVU	Total Vertical Uncertainty
NOAA	National Oceanic and Atmospheric Association
PPP	Precise Point Positioning
MLLW	Mean Lower Low Water
HTDP	Horizontal Time-Dependent Positioning Tool
SABER	Survey Analysis and Area-Based Editor
EGM2008	Earth Gravitational Model 2008
CHS	Canadian Hydrographic Service
MRP	Master Reference Point
IMU	Inertial Measurement Unit
CD	Chart Datum
LLWLT	Lowest Low Water, Large Tide
DFT	Discrete Fourier Transform
IDFT	Inverse Discrete Fourier Transform

Abstract

One challenge for Autonomous Underwater Vehicle (AUV) multibeam surveying is the limited ability to assess internal vertical agreement rapidly and reliably. Applying an external ellipsoid reference to AUV multibeam data would allow for field comparisons. A method is established to merge ellipsoid height (EH) data collected by a surface vessel in close proximity to the AUV. The method is demonstrated over multiple collection missions in two separate areas. Virtual tide corrector values are derived using EH data collected by a boat and a measured ellipsoid to chart datum separation distance. Those values are compared to measurements by a traditional tide gauge installed nearby. Results from the method had a mean difference of 6 centimeters with respect to conventional data and had a mean total propagated uncertainty of 15 centimeters at the 95% confidence interval. Methodologies are examined to characterize their accuracies and uncertainty contribution to overall vertical correction.

Keywords: AUV, tides, GNSS, hydrography, virtual tide corrector, uncertainty

I. Introduction

Autonomous Underwater Vehicles (AUVs) are an increasingly important tool for the collection of hydrographic data (Hiller, Steingrimsson, and Melvin 1). While the benefits of using AUVs for data collection are numerous, they are of little importance if the data collected have too large a positional uncertainty to meet the requirements of the hydrographic products they will be supporting. Tide offsets are one of the largest sources of uncertainty in hydrographic data, and although traditional observation of tidal fluctuation near the survey area can account for changes and reduce this uncertainty, operational constraints often prevent continuous and local tidal observations (Brennan et al. 1). Applying an ellipsoid reference to AUV multibeam data would achieve the same purpose without the need to collect conventional, observed tides, but a significant challenge exists in that an underwater vehicle cannot collect ellipsoid height (EH) data directly. This thesis establishes techniques of collecting these data from nearby surface vessels and then using those data to derive a time series of virtual water level values. Those techniques allow in field assessment and comparison of data with other collection platforms. This research examines methodology, accuracy, and vertical uncertainty of this technique for generating virtual water level measurements using EH collected from a nearby surface vessel.

II. Background

Establishing and using an ellipsoid-based vertical reference for hydrographic data is of particular interest to the modern hydrographer. It has been thoroughly established that the essential components of applying an ellipsoid reference include antenna positioning, translation to the water surface, and transformation to a reference datum (Dodd et al. 2). Techniques have been developed for accomplishing these components using the survey vessel itself as the tie-in to the ellipsoid (Rice and Riley 2). Numerous iterations of testing and experience by many organizations have resulted in standard operating procedures (SOP) that maximize effectiveness and minimize and quantify uncertainty (Dodd and Mills 2).

Wert has examined the suitability of a particular Global Navigation Satellite System (GNSS) receiver as for the retrieval of tidal heights but did so using zero-mean comparisons of EH measurements and echosounder depth measurements from a vessel frozen in land-fast sea ice (92-101). This thesis demonstrates a workflow for calculating a tide corrector using GNSS EH measurements collected by mobile vessels and adjusting those measurements to a true vertical datum. Mean differences will be examined after vertical datum adjustment because their effect on overall depth measurement will be significant. What's more, the ability to collect measurements from a mobile platform is essential considering that the resulting correctors must be applicable to AUVs that will not always be collecting bathymetric data in the same location.

Although it is generally agreed upon that the problems of surveying with AUVs share a great deal in common with other modes of hydrographic survey, little information exists on the design of techniques intended for chiefly underwater vehicles. This research effort intends to examine one such technique's applicability to an AUV-centric concept of operations as well as to ensure adequate uncertainty management in the process. This technique has the advantages of

using equipment already being employed and having inputs and outputs that fit well into the preexisting processing stream for AUV hydrographic data collection.

III. Proposed Solution

Applying a water level corrector derived from EH measurements to AUV multibeam data could result in significantly lower overall vertical uncertainty compared to applying water level correctors from predicted tides. It would also reduce the required data collection effort compared with applying corrections via observed tides. In particular, shore-based gauge installation would not be necessary during data collection activities except as required to validate modeled values for the ellipsoid to chart datum separation (SEP) (Dodd et al. 12). Although determining the SEP requires a combination of measurement and modeling, such determination can be made once and used again throughout subsequent surveys in the same area. Depending on the requirements driving the multibeam data collection, it is possible that only relative vertical alignment of multiple survey lines is essential. In that case, any SEP model lacking sharp, local discontinuities in the area of interest would provide the input needed to obtain relative vertical alignment.

Once the SEP is known, the chief requirement of deriving virtual tide corrector values is a continuous, concurrent source of EH data. For surface vessels equipped to collect GNSS data, this source is readily available. Because an AUV is a submerged vehicle, using on-board GNSS collection capabilities is not an option. However, if a surface vessel were to remain close enough to the horizontal position of the AUV such that the relative changes in water level at the location of the surface vehicle and the (horizontal) location of the AUV were negligible, then that surface vessel could supply the continuous EH source needed for this technique. The surface vessel could be a ship, a small boat, a GNSS buoy, or an autonomous surface vehicle (ASV). This research involved two primary data collection efforts. The first of these collections occurred on *Meriel B.,* a 50-foot work boat owned by Hydroid, LLC and built by Millennium Marine. For the

second collection, the Naval Oceanographic Office's (NAVOCEANO's) Hydrographic Survey Launch (HSL) number 16 (a 34-foot survey boat) was used.

Figure 1 depicts the derivation and makeup of a conventional tide corrector for AUV multibeam data.

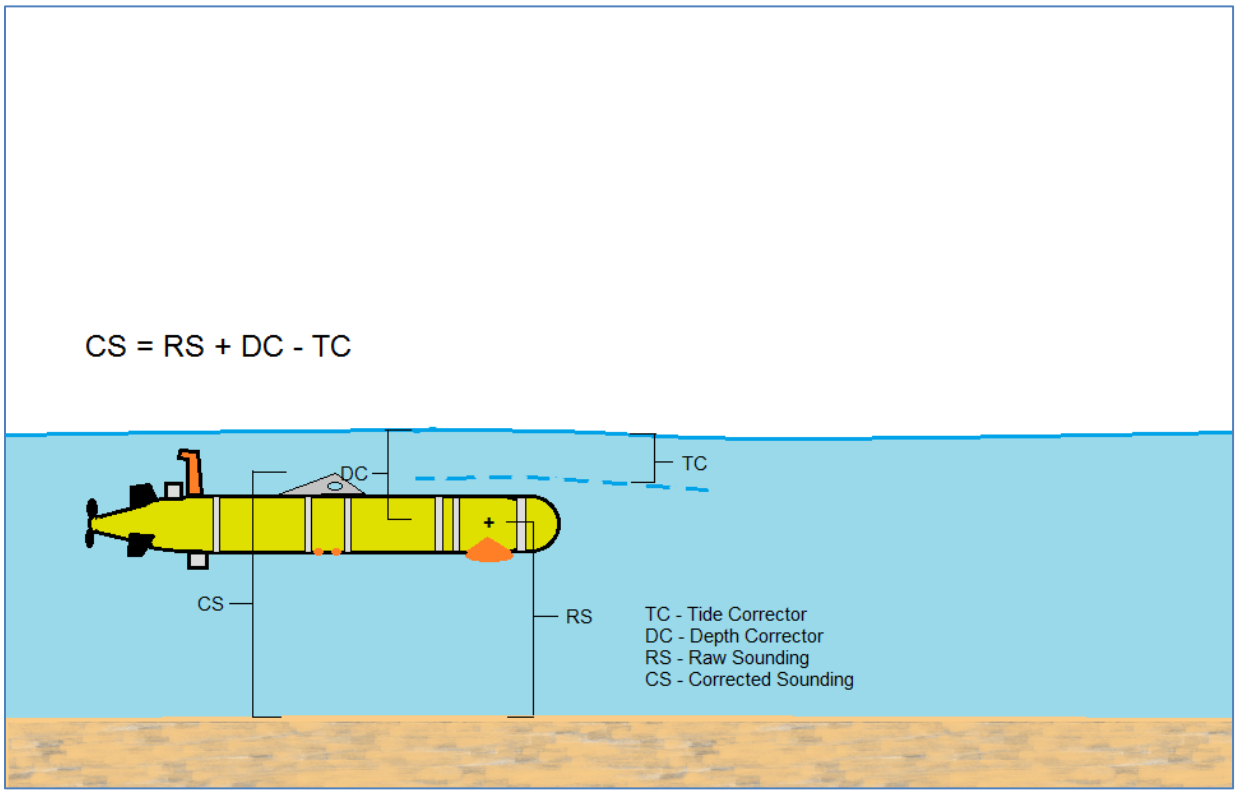

Figure 1 – Diagram of conventional AUV water level correction with vertical locations of Tide Corrector, Depth Corrector, Raw Sounding, and Corrected Sounding indicated.

Figure 2 depicts the derivation and makeup of a virtual tide corrector (VTC) for AUV multibeam data. Note that the terms contributing to the corrected sounding (highlighted in purple) are equivalent to the VTC, which contributes to the corrected sounding in the same way as the conventional tide corrector depicted in Figure 1.

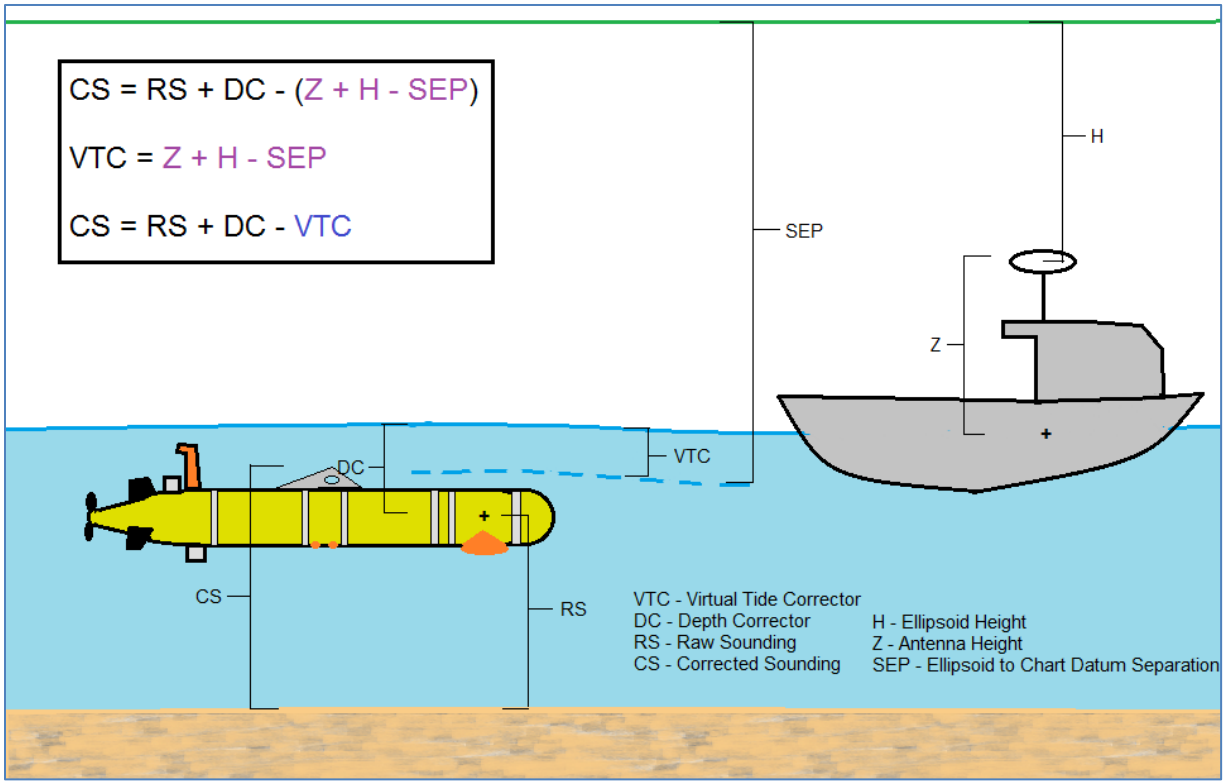

Figure 2 – Diagram of virtual AUV water level correction with ellipsoid in green and vertical locations of VTC, Depth Corrector, Raw Sounding, Corrected Sounding, Ellipsoid Height, Antenna Height, and Ellipsoid to Chart Datum Separation indicated.

The accuracy of a method for obtaining VTCs can be determined by comparing those correctors with observed, conventional tidal elevations from the same area collected at the same. The horizontal extents of the applicability of this technique will doubtlessly be the subject of future work, but for the purposes of this research, all EH data were collected 7 nautical miles or less from the conventional gauge, and data were not segregated with respect to distance from the tide gauge. Collection areas were chosen such that there was always a clear path (free of topographical interruption) from the vessel to the tide gauge. The VTC was computed for all times where EH data were collected, and a difference between the virtual corrector and a conventional corrector were computed for all overlapping times.

The estimation of the uncertainty in such a method can be accomplished by examining the uncertainties of all input parameters to the method as well as their mechanism of contribution

to the vertical component. The uncertainty of the method is of particular interest to the hydrographic community because of the contribution to the overall vertical (and total) uncertainty in corrected sounding data. Specifically, if it can be shown that the technique can result in uncertainties of a similar magnitude to those resulting from conventional tide correction, then the decision to operationally use the technique can be made with much greater confidence.

The International Hydrographic Organization (IHO) sets maximum allowable positional uncertainty standards for hydrographic surveys to help improve safety of navigation. Total vertical uncertainty (TVU) describes the vertical component of these uncertainty standards as it is propagated throughout all influencing measurements (e.g., EH, antenna height above the waterline). Allowable TVU is a function of total water depth and differs depending on the Order (stringency) specified for a given survey (IHO S-44). At NAVOCEANO, for example, AUVs are used to conduct IHO Order 1a or Order 1b surveys, and the allowable TVU for those surveys is calculated by

$$TVU = \sqrt{0.5^2 + (0.013 * depth)^2}$$

(3.1)

AUVs will most often operate in 50 – 400 meters of total water depth, which corresponds to 82-114 centimeters of allowable TVU at the 95% confidence interval (i.e., 2 standard deviations). As those standards represent a minimum acceptable level, it is important that this technique minimize uncertainty wherever possible. This minimization is important because tide correction is one of the largest contributors to overall vertical uncertainty and because multiple other factors' uncertainties (e.g., refraction effects, motion measurement error) must also fit within that limit. A yield of additional uncertainty less than 20 centimeters at 2 standard deviations (corresponding to approximately 10 centimeters at 1 standard deviation and representing

approximately 25% of the Order 1 allowable TVU for 50 meters of total water depth) would represent strong viability of the technique for use in IHO Order 1 hydrographic surveys.

IV. Methods

A. First Collection Period

The first data collection period occurred as a part of University of New Hampshire's and University of Delaware's AUV Boot Camp from August 4 to August 6, 2014. For this workshop, Hydroid, LLC used *Meriel B.* to deploy and recover a REMUS 600 AUV, so *Meriel B.* was chosen as the surface vessel from which EH data would be collected. A C-Nav3050 GNSS receiver was installed in the cabin of *Meriel B.* The receiver was connected to a cabin-top-mounted NavCom Technology, Inc. ANT-3001R rover antenna measured at 3.78 meters above the waterline. This measurement was obtained using a tape measure and is expected to be accurate within 3 centimeters. Note that this 3-centimeter uncertainty does not include the effects of squat and loading. (i.e. – The measurement is expected to be 3.78 meters +/- 3 centimeters under a certain set of loading conditions and no squat effects.) Antenna placement was chosen to maximize satellite visibility without the need for special equipment or undue human risk during installation. Mounting the antenna in a temporary fashion allowed for efficient installation and breakdown while limiting movement of the antenna to less than 1 centimeter in any direction. The reductions in antenna height above the waterline caused by roll, pitch, and settlement were neglected for this part of the test period and will be the subject of later discussion. The horizontal displacements arising from roll, pitch, and yaw effects are sufficiently small in comparison with the horizontal distance between *Meriel B.* and the tide gauge such that they were disregarded for this data collection period.

Navigation data were collected at 1-second intervals on local storage onboard the C-Nav3050 receiver extending at least 30 minutes before and after multibeam data collection. The receiver was powered on pierside and not powered off until the boat had returned, so the data

collection always included transit legs to and from the survey areas. Navigation and water level data were collected for 6, 8.5, and 7 hours on each of the three survey days, respectively. Weather conditions were largely calm for all data collection periods, never exceeding Douglas sea state 3 and rarely exceeding Douglas sea state 2.

A National Oceanic and Atmospheric Administration (NOAA) tidal gauge (Station ID 8423898) collected data throughout the surveys and provided water elevation data at 6-minute intervals. Observed, verified tides for all times were downloaded on February 9, 2015. During the first two days, the survey areas were 11 to 13 kilometers east of the tide gauge. During the third day, the survey area was 1 to 2 kilometers east of the tide gauge.

Raw GNSS data collected by the C-Nav3050 receiver on *Meriel B.* were downloaded daily. The GNSS data were combined with clocks and rapid ephemerides data from the University of Bern's Center for Orbit Determination in Europe and were processed using Waypoint GraphNav to provide a Precise Point Positioning (PPP) solution of antenna height with respect to the ellipsoid and antenna geographical location. PPP is a method of increasing precision in position determination without the need for an additional GNSS receiver. It uses code and phase information observed by a dual-frequency receiver and combines them with satellite clock and ephemeris data to minimize some of the most significant error sources in GNSS position. As a result, it reduces the overall positional uncertainty of the processed solution (Gao 16-18).

For this experiment the geographical portion of the PPP solution was discarded. For the antenna position to be reduced to the waterline exactly, both antenna offsets from a rotation center and vessel attitude must be taken into account. However, *Meriel B.* was not equipped with a motion sensor. Therefore, the horizontal displacement of the antenna from a rotation point can

be ignored. To account for the measured height of the antenna above the waterline, the height data were reduced by 3.78 meters.

The VTC was calculated for each waterline-corrected EH by taking the difference of the height and the SEP (i.e., the distance from the ellipsoid to the vertical datum of Mean Lower Low Water (MLLW)) at that point. Tidal datums have many applications, among which is the provision of a vertical reference to which observed water depths can be referred (National Oceanic and Atmospheric Administration 1). Byrne, et al. used NOAA's Horizontal Time-Dependent Positioning tool (HTDP) to compute the SEP for that datum to be –29.32 meters at the NOAA tide gauge during work completed during the Shallow Survey 2008 conference (9). Table 1 includes the benchmark measurements determined during that conference and used in SEP grid creation for the first collection period.

Table 1 – Horizontal and vertical locations of benchmarks used to generate SEP grid for AUV Boot Camp 2014.

Latitude	Longitude	To Ellipsoid (m)	To MLLW (m)	SEP (m)
43° 4' 13.1679" N	70° 42' 39.1271" W	-23.306	6.009	-29.315
43° 4' 15.1738" N	70° 42' 48.5872" W	-20.445	8.879	-29.324

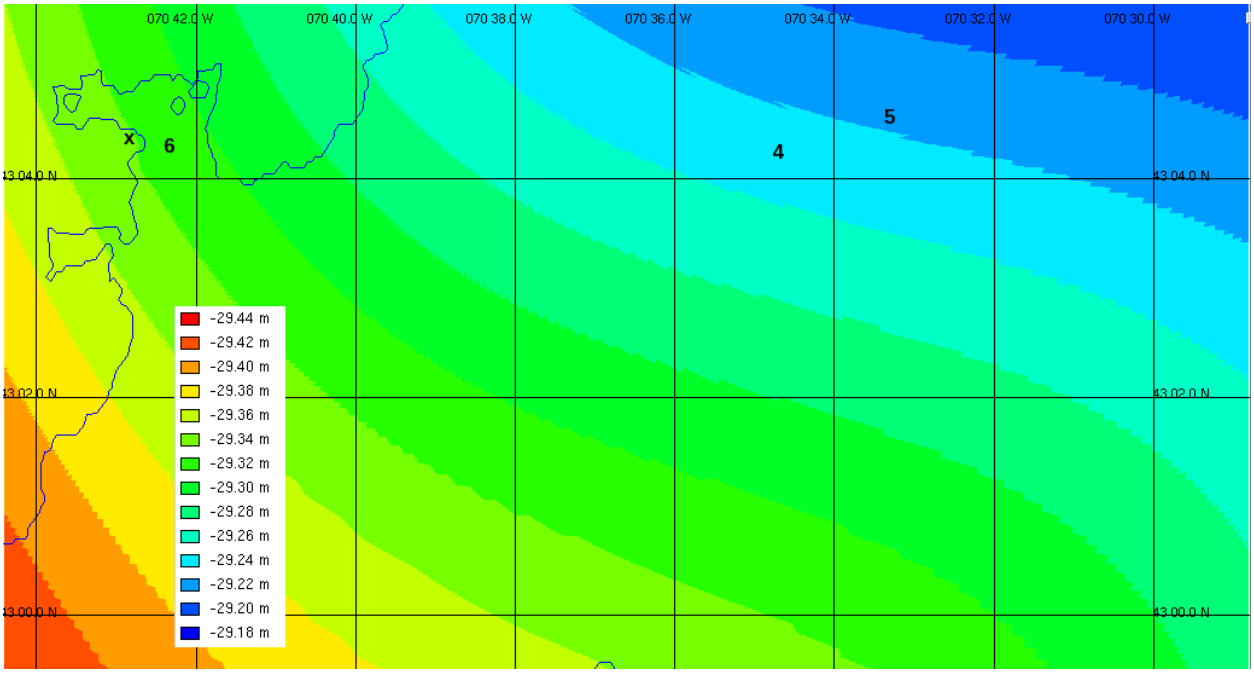

Figure 3 – SEP grid and legend for AUV Boot Camp 2014. Tide gauge marked with X. Centers of survey areas for August 4, 5, and 6 marked with 4, 5, and 6, respectively.

That benchmark information was processed using Leidos' Survey Analysis and Area-Based Editor (SABER) and combined with the National Geospatial-Intelligence Agency's Earth Gravitational Model 2008 (EGM2008) to generate a calibrated SEP grid for the entire (3-day) area. That SEP grid, the tide gauge location, and the center of each day's survey areas are depicted in Figure 3. The calibrated SEP surface is generated using EGM2008 as an initial condition for a SEP grid and warping the grid to known or measured SEP values at one or more control points. Each EH measurement was reduced to the waterline, and the SEP value at that horizontal location was subtracted to give a VTC value for that instantaneous measurement. The finer resolution vertical solution was averaged to a one-minute time interval for the creation of a VTC to MLLW for each position. Figure 4 depicts this portion of the processing stream for data collected during AUV Boot Camp 2014.

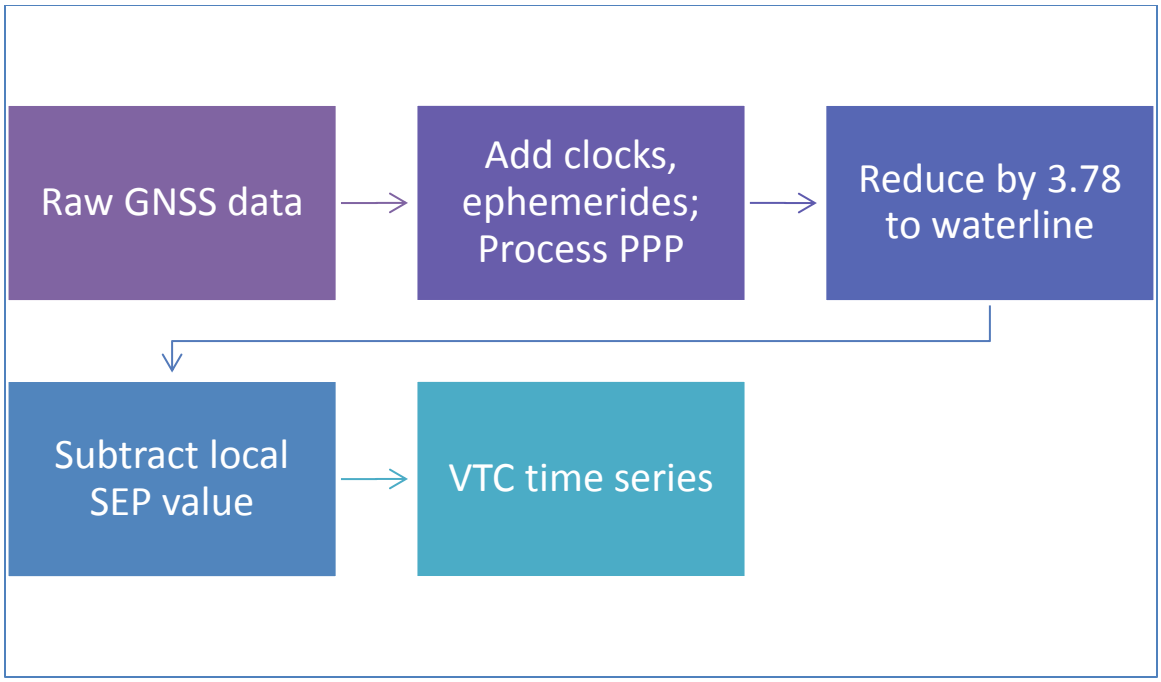

Figure 4 – Diagram of processing stream for Meriel B. VTC data from AUV Boot Camp 2014.

B. Second Collection Period

For the second collection period, NAVOCEANO was performing acceptance and readiness testing on several AUVs and HSL 16 in Sidney, British Columbia, Canada from June to August 2015. This testing was performed in partnership with the Canadian Hydrographic Service (CHS), a division of the Science Branch of the Department of Fisheries and Oceans Canada. On June 27 and July 4 through 8 of that test period, HSL 16 operated in Patricia Bay and Saanich Inlet. Because it was available and operating near a shore-based tide gauge, HSL 16 was chosen as the vessel from which EH data would be collected. HSL 16 was equipped with a NavCom 3050 GNSS receiver connected to a cabin-top-mounted AN-2004T antenna surveyed in at 2.10 meters aft of the master reference point (MRP), 0.03 meters port of the MRP, and 2.25 meters above the MRP. The MRP vertical location is approximately 0.57 meters below the waterline, although dynamic draft factors will inevitably cause this value to vary at least slightly. The MRP is the location on HSL 16 from which all survey measurements are commonly referenced. It is approximately the point about which the vessel will rotate from roll, pitch, and turning; however, this rotation center is not exactly static, and its variability will be the subject of later discussion. Unlike the setup for *Meriel B.*, HSL 16's setup is rigidly and permanently mounted and is expected not to move to any appreciable degree, and its antenna offset values are expected to be accurate within 0.02 meters each. Weather conditions were largely calm for all data collection periods, rarely exceeding Douglas sea state 2.

A CHS tidal gauge (Station ID 7277) was located on the shoreline of Patricia Bay near the pier adjacent to the Institute of Ocean Sciences. It collected data throughout the surveys and provided water elevation data at 1-minute intervals for those periods. Observed, verified tides for

all times were downloaded on July 18, 2015. All survey areas were limited to Saanich Inlet and Patricia Bay and within 8 kilometers of the tide gauge.

PPP navigation data were generated in the same manner as the AUV Boot Camp data. Again, for this experiment, the geographical portion of the PPP solution was discarded. Because this vessel came equipped with motion sensing equipment, it was decided that the EH data would be reduced by an antenna height calculated from surveyed antenna offsets and real-time attitude measurements. An Applanix POS-MV Version 5 inertial measurement unit (IMU) collected attitude information for HSL 16 at a frequency sufficient to provide attitude information much denser than the navigation requires. Its angular measurements are expected to be accurate to within 0.02 degrees for roll and pitch and 0.01 degree of heading.

Diebel shows that the function that maps a vector of Euler angles to its rotation matrix is

$$R_{XYZ} = \begin{bmatrix} cos\beta\ cos\gamma & cos\beta\ sin\gamma & -sin\beta \\ cos\gamma\ sin\alpha\ sin\beta - cos\alpha\ sin\gamma & cos\alpha\ cos\gamma + sin\alpha\ sin\beta\ sin\gamma & cos\beta\ sin\alpha \\ cos\alpha\ cos\gamma\ sin\beta + sin\alpha\ sin\gamma & cos\alpha\ sin\beta\ sin\gamma - cos\gamma\ sin\alpha & cos\alpha\ cos\beta \end{bmatrix}.$$

(4.1)

where α is roll and is positive when the starboard side moves downward, β is pitch and is positive when the bow moves up, and γ is yaw and is positive when the bow turns to starboard (Diebel 11). Weisstein shows in his article on rotation matrices that for a given point A_X, A_Y, and A_Z meters in the positive directions along the X, Y, and Z axes, respectively, from the MRP when the system experiences zero roll, pitch, and yaw, the point's displacement from the MRP under any roll, pitch, and yaw is

$$\begin{bmatrix} A_X{}' \\ A_Y{}' \\ A_Z{}' \end{bmatrix} = R_{XYZ} * \begin{bmatrix} A_X \\ A_Y \\ A_Z \end{bmatrix}.$$

(4.2)

The new displacement of the antenna from the MRP in the z direction is then

$$A'_Z = A_X(cos\alpha\ cos\gamma\ sin\beta + sin\alpha\ sin\gamma) + A_Y(cos\alpha\ sin\beta\ sin\gamma - cos\gamma\ sin\alpha) + A_Z cos\alpha\ cos\beta.$$

(4.3)

For this configuration on HSL 16, the z displacement is

$$A'_Z = -2.10(cos\alpha\ cos\gamma\ sin\beta + sin\alpha\ sin\gamma) + -0.03(cos\alpha\ sin\beta\ sin\gamma - cos\gamma\ sin\alpha) + -2.55 cos\alpha\ cos\beta.$$

(4.4)

From the MRP-corrected height, the waterline corrected height was obtained by adding the waterline value (positive when the waterline is below the MRP).

The VTC was calculated for each waterline-corrected EH by taking the difference of the height and the ellipsoid to the Chart Datum (CD) SEP in the area. Note that CD for this area very closely approximates but is not identical to lowest low water, large tide (LLWLT). A representative from CHS provided both ellipsoid to geoid and geoid to CD differences for the aforementioned tide gauge and three other nearby stations, and those data are included in Table 2.

Table 2 – Horizontal and vertical locations of benchmarks used to generate SEP grid for HSL 16 during the 2015 testing period.

Latitude	Longitude	To Ellipsoid (m)	To CD (m)	SEP (m)
48° 38' 51.6696" N	123° 23' 36.6072" W	-18.967	2.027	-20.994
48° 39' 8.6472" N	123° 26' 53.7756" W	-18.706	2.108	-20.814
48° 48' 56.5272" N	123° 36' 34.8588" W	-18.171	2.390	-20.561
48° 46' 7.5432" N	123° 26' 57.8184" W	-18.791	2.082	-20.873

That benchmark information was processed as before using SABER and combined with the EGM2008 to generate a calibrated SEP grid for the entire area. Figure 5 depicts the SEP grid generated by SABER.

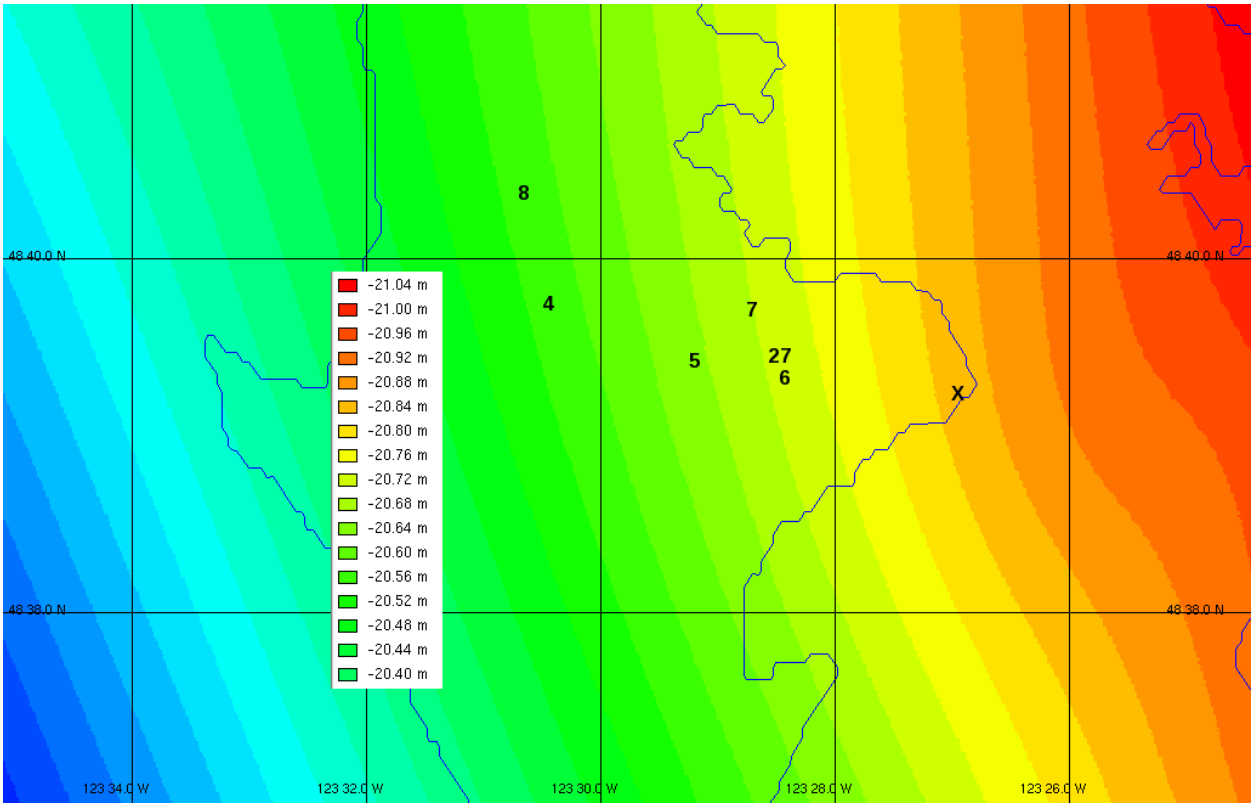

Figure 5 – SEP grid and legend for HSL 16 2015 testing period. Tide gauge marked with X. Centers of survey areas for June 27 and July 4, 5, 6, 7, and 8 marked with 27, 4, 5, 6, 7, and 8, respectively.

The horizontal location was located on the SEP grid, and the SEP value at that grid cell was subtracted to give a VTC value for each instantaneous GNSS measurement. The finer resolution vertical solution was averaged to a one-minute time interval for the creation of a VTC to CD for each position. Figure 6 depicts this portion of the processing stream for data collected by HSL 16 during the 2015 test period.

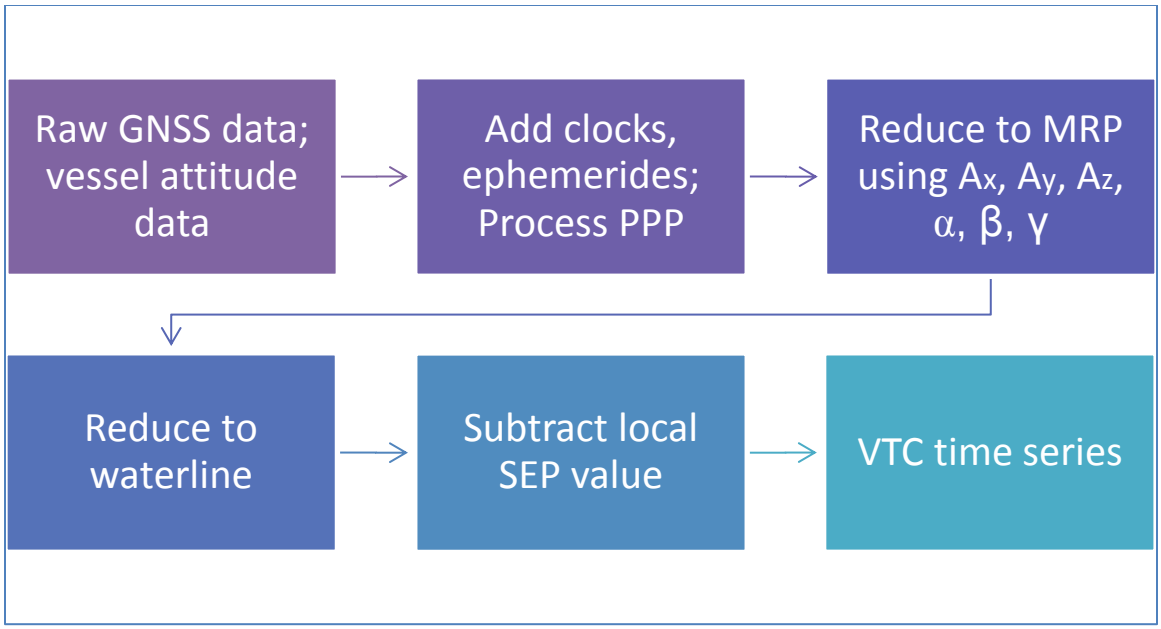

Figure 6 – Diagram of processing stream for HSL 16 VTC data from 2015 test period.

C. Common Processing

The processing stream from this point was the same for both collection periods. Comparing each VTC dataset with its concurrent conventional tide corrector dataset demonstrated both that general agreement existed between the datasets and that significantly more noise existed in each VTC dataset than its conventional counterpart. Low-pass filtering of the VTC data would remove the effects of small motions of the surface vessel while retaining the long-term effects of changing water levels. For straightforwardness and robustness, filtration in the frequency domain was chosen to accomplish the low-pass filtering (Press et al. 558). GNU Octave version 3.6.1 was used to perform a discrete Fourier transform (DFT) on the data and multiply by the following filter function:

$$H(s) = \begin{cases} 1 & for \quad 0 \le s < \frac{N}{20} \\ 1 - \frac{\left(s - \frac{N}{20}\right)}{\frac{N}{20}} & for \ \frac{N}{20} \le s < \frac{N}{10} \\ 0 & for \ \frac{N}{10} \le s < \frac{9\,N}{20} \\ \frac{s - 9\,N}{20N} & for \ \frac{9\,N}{20} s \le \frac{N}{2} \end{cases}$$

(4.5)

Because the sampling period was one minute (1/60 hz), the frequency specified by each element of the filter function was

$$f = \frac{s}{60N} hz.$$

(4.6)

Thus, the frequency bands between

$$\frac{1}{1200}hz \leq f < \frac{1}{600}hz$$

(4.7)

and

$$\frac{10}{1333}hz \leq f < \frac{1}{120}hz$$

(4.8)

are attenuated and

$$\frac{1}{600}hz \leq f < \frac{10}{1333}hz$$

(4.9)

are eliminated. The high frequency limit of the filter (corresponding to a 2-minute period) was chosen to coincide with the Nyquist frequency (Weisstein Nyquist). The starting point (corresponding to a 20-minute period) was chosen so as to remove the effects whose periods were small but retain the long-term tidal effects. The shape of the tapering at the ends of the filter function was chosen to provide some leakage protection while mitigating any compromise in resolution (Bracewell 281).

Octave was then used to apply an inverse DFT to the data. Removal of higher frequency noise in the frequency domain has been shown to be effective on similar data types (Riley and Murray 4). The processed VTC data showed much better agreement with the conventional data but still exhibited sharpness that was absent in the conventional data. Octave was used to apply pseudo-Gaussian (convolution) smoothing using a window of 30 minutes' length. This window size was chosen empirically after visual evaluation of the effects of various window lengths on the shape of the VTC curve. This smoothing was applied to each continuous interval of VTC data and resulted in data that were much more representative of actual tidal changes and less

reflective of the small motions experienced by the surface vessel yet not affecting any potential subsea collection platform. Figure 7 depicts this portion of the processing stream, which was used for data from both collection periods.

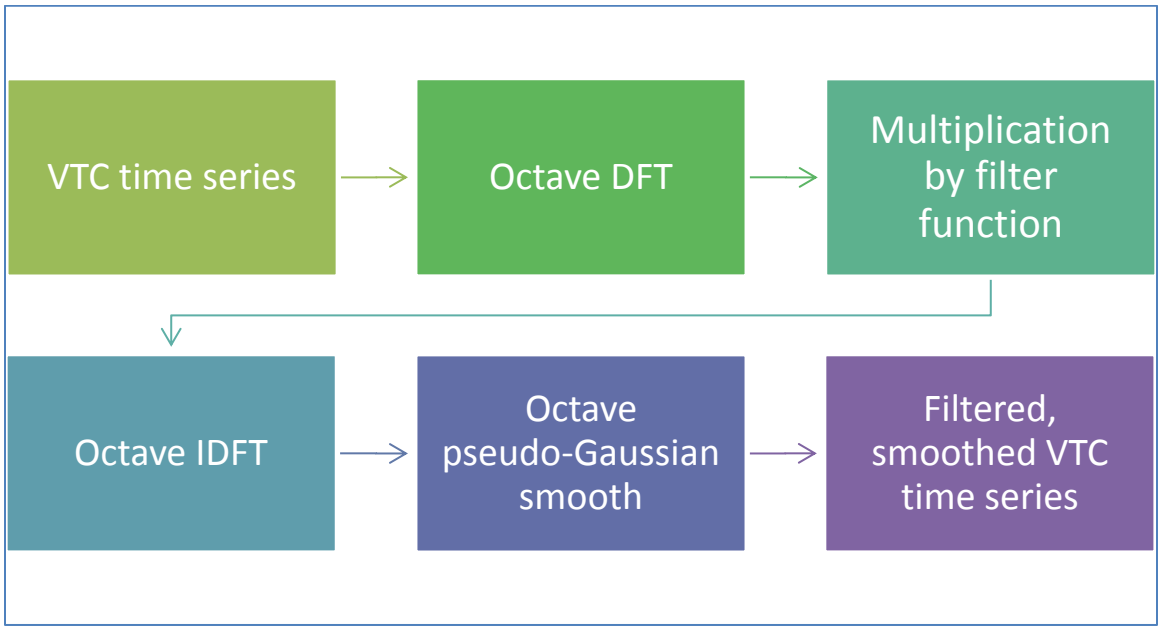

Figure 7 – Diagram of common processing stream for both collection periods.

Figure 8 depicts a sample of the VTC data at the three stages of smoothing: unsmoothed, frequency domain filtered, and pseudo-Gaussian smoothed.

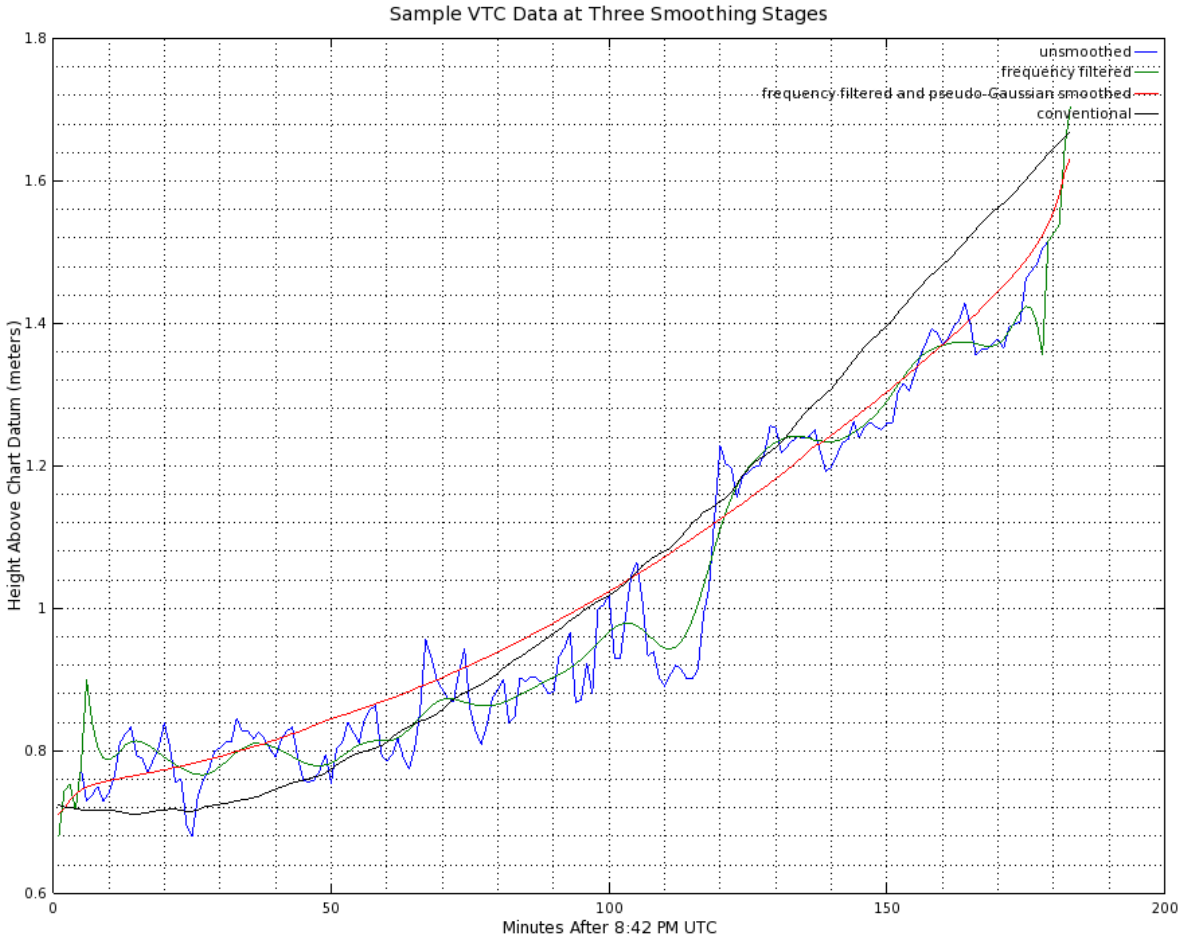

Figure 8 – Example of VTC data at three stages of smoothing. Unsmoothed VTC data in blue, frequency filtered data in green, pseudo-Gaussian smoothed, frequency filtered data in red, and conventional tide data in black.

At this stage of processing, the VTC data have the same format as conventionally measured water level data commonly used to correct bathymetric data. The time series of water height above a particular datum (MLLW or CD in these two collection periods) are subtracted from the measured sounding depth to give the depth corrected as though it had been collected when the water level was at that datum. The VTC data can then be applied to AUV bathymetric data using SABER's *saber_apply_tides* routine or one of many other software programs.

It would require substantially more investigation to directly compare bathymetric data that had been conventionally corrected with data corrected via VTC, and since tide correction is a simple, arithmetic process, it follows that tide correctors that compare well with a given standard would result in bathymetric data whose comparisons would behave similarly well.

V. Uncertainty

A. First Collection Period

For the first collection period, it is difficult to quantify the uncertainty of the VTC data due to the lack of vessel attitude data. With assumptions (a) that roll and pitch rotation of the vessel occurred about the waterline, (b) that the GNSS antenna was mounted on the centerline ($A_Y = 0$), (c) that the antenna was mounted 2 meters forward of the rotational center, and (d) that roll and pitch are limited to 0.085 radians in either direction, an approximate range of uncorrected vertical displacement can be determined using (4.3). Because of assumption (b), that equation simplifies to

$$A'_Z = 2.00(cos\alpha\ cos\gamma\ sin\beta + sin\alpha\ sin\gamma) - 3.78(cos\alpha\ cos\beta).$$

(5.1)

Table 3 describes the conditions (under the aforementioned constraining assumptions) under which extrema are observed:

Table 3 – Maximal and minimal conditions and resulting values for Δz for Meriel B., with assumptions.

Roll (rad)	Pitch (rad)	Yaw (rad)	Condition	Drop (m)
+/-0.085	0.085	π	Maximum	-3.58
+/-0.085	-0.085	0	Maximum	-3.58
0	0.085	0	Minimum	-3.94
0	-0.085	π	Minimum	-3.94

Those extrema would contribute to differences of 16 and 20 centimeters with respect to the value used for calculating VTCs. For lack of a more concrete approach, the arithmetic mean of those two differences (0.18 meters) will be used to estimate the uncertainty in the VTC due to uncertainty in vessel attitude ($s_{A_Z'}$). This uncertainty should be considered along with those resulting from GNSS measurement (s_{GNSS}) and SEP value calculation (s_{SEP}). According to the

formula used by Ku for the propagation of error in non-correlated variables, the variance of the VTC measurement is

$$(s_{VTC})^2 = (s_{A_Z'})^2 + (s_{GNSS})^2 + (s_{SEP})^2$$

(5.2)

when all contributing parameters affect the result linearly as they do in this case (Ku 267). The value for s_{GNSS} is reported with each post-processed GNSS measurement obtained from Grafnav, and s_{SEP} was determined by SABER as 0.01 meters throughout the survey area. As a result, the uncertainty for each VTC measurement from the first collection period can be calculated by

$$s_{VTC} = \sqrt{0.18^2 + 0.01^2 + (s_{GNSS})^2}$$

(5.3)

B. Second Collection Period

The presence of vessel attitude data for the second collection period allowed for significantly more rigorous quantification of uncertainty, especially for the vertical displacement from the antenna to the waterline. The components of s_{GNSS} and s_{SEP} contribute in the same way as in the first collection period. When the components of $s_{A_Z'}$ are known and when the new displacement of the antenna from the MRP on the z axis is as described in equation (4.3), a more general version of Ku's aforementioned formula in (5.2) becomes

$$(s_{A_Z'})^2 = (\frac{\partial A_Z'}{\partial A_X} s_{A_X})^2 + (\frac{\partial A_Z'}{\partial A_Y} s_{A_Y})^2 + (\frac{\partial A_Z'}{\partial A_Z} s_{A_Z})^2 + (\frac{\partial A_Z'}{\partial \alpha} s_{\alpha})^2 + (\frac{\partial A_Z'}{\partial \beta} s_{\beta})^2 + (\frac{\partial A_Z'}{\partial \gamma} s_{\gamma})^2$$

(5.4)

Taking partial derivatives from (4.3) gives

$$\frac{\partial A_{Z'}}{\partial A_X} = cos\alpha\ cos\gamma\ sin\beta + sin\alpha\ sin\gamma,$$

(5.5)

$$\frac{\partial A_{Z'}}{\partial A_Y} = cos\alpha\ sin\beta\ sin\gamma - sin\alpha\ cos\gamma\ ,$$

(5.6)

$$\frac{\partial A_{Z'}}{\partial A_Z} = cos\alpha\ cos\beta,$$

(5.7)

$$\frac{\partial A_{Z'}}{\partial \alpha} = A_X(cos\alpha\ cos\gamma - sin\alpha\ sin\beta\ cos\gamma) + A_Y(-sin\alpha\ sin\beta\ sin\gamma - cos\alpha\ cos\gamma) - A_Z sin\alpha\ cos\beta,$$

(5.8)

$$\frac{\partial A_{Z'}}{\partial \beta} = A_X \cos\alpha \cos\beta\ cos\gamma + A_Y cos\alpha\ cos\beta\ sin\gamma - A_Z sin\alpha\ cos\beta, \text{ and}$$

(5.9)

$$\frac{\partial A_{Z'}}{\partial \gamma} = -A_X\,(\cos\alpha \sin\beta\, sin\gamma + \sin\alpha\, cos\gamma) + A_Y(cos\alpha\, sin\beta\, cos\gamma + sin\alpha\, sin\gamma),$$

(5.10)

Substituting in the antenna offsets, antenna offset uncertainties, and angular measurement uncertainties described in Section IV, Subsection B with (5.5-10) gives

$(s_{A_{Z'}})^2 = 0.02^2 * [(cos\alpha\, sin\beta cos\gamma + sin\alpha\, sin\gamma)^2 + (cos\alpha\, sin\beta\, sin\gamma - sin\alpha\, cos\gamma)^2 + (cos\alpha\, cos\beta)^2] + 0.02^2$ [-2.10* $(cos\alpha\, cos\gamma + sin\alpha\, sin\beta\, cos\gamma)$ -0.03*$(-cos\alpha\, cos\gamma - sin\alpha\, sin\beta\, sin\gamma) + 2.55\, sin\alpha\, cos\beta]^2 + 0.02^2[2.10\, cos\alpha\, cos\beta\, cos\gamma - 0.03\, cos\alpha\, cos\beta\, sin\gamma + 2.55\, sin\alpha\, cos\beta]^2 + 0.01^2[-2.10(sin\alpha\, cos\gamma + cos\alpha\, sin\beta\, sin\gamma) + 0.03(sin\alpha\, sin\gamma + cos\alpha\, sin\beta\, cos\gamma)]^2$.

(5.11)

With the assumption a 5-centimeter uncertainty for the displacement from the MRP to the waterline (s_{WLZ}), and since SABER reported s_{SEP} to be 0.01 throughout the survey area as with the first collection period, the overall uncertainty is given by

$$s_{VTC} = \sqrt{0.05^2 + 0.01^2 + (s_{GNSS})^2 + (s_{A_{Z'}})^2}$$

For each collection period, these uncertainties have been maintained and propagated throughout the data flow and are displayed in Section VI, Results.

VI. Results

Comparisons of virtual and conventional tide correctors were examined for each of three days in the first collection period and six days in the second collection period with totals of 1,372 and 1,647 minutes of comparisons, respectively. For these results, a positive mean or median signifies a VTC value larger than (higher above MLLW or CD) the conventional corrector. Figure 9 depicts the overall statistics of the differences for each collection day.

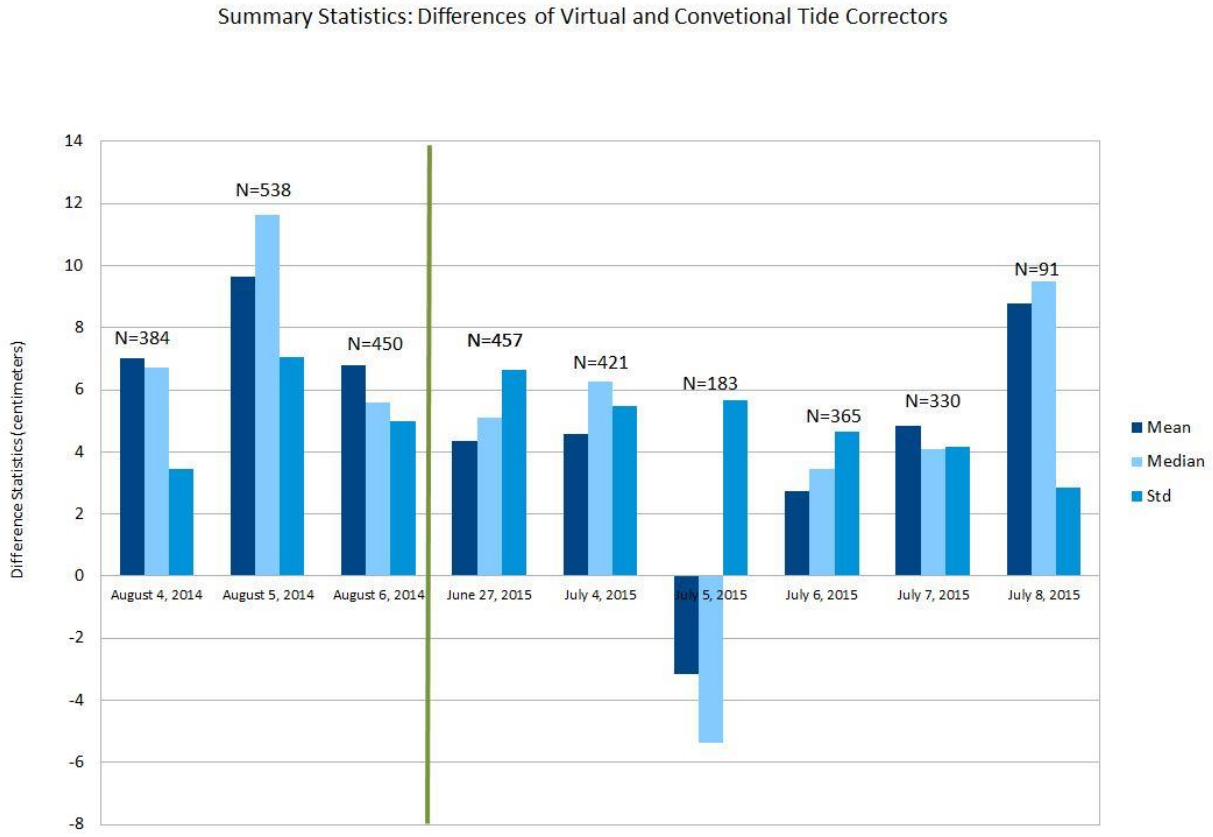

Figure 9 – Summary statistics of differences from all nine collection days.

The overall median and mean values were almost exclusively positive with the exception of July 5. The largest differences were observed during the first collection period; however, standard deviation values for that period were not drastically larger than values from the second collection period. Below are the results from each test day depicted in Figures 10-18.

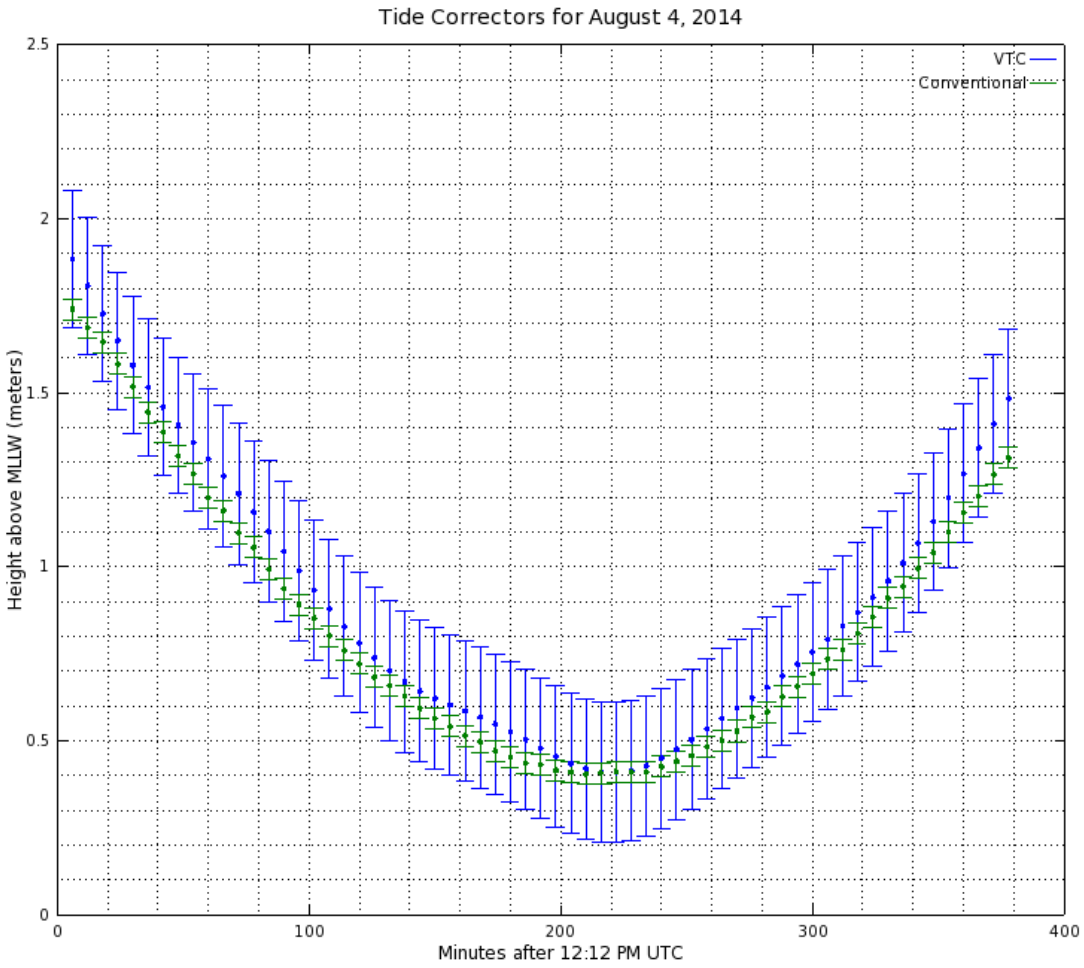

Figure 10 – Tide Correctors for August 4, 2014.

The VTCs for August 4 approximate the shape of the conventional tide curve very well. The overall bias of 7 centimeters is apparent, and the difference is larger at the end of the flood period compared to the rest of the collection day. For all periods, the conventional data were considerably within the lower uncertainty limits of the VTC data.

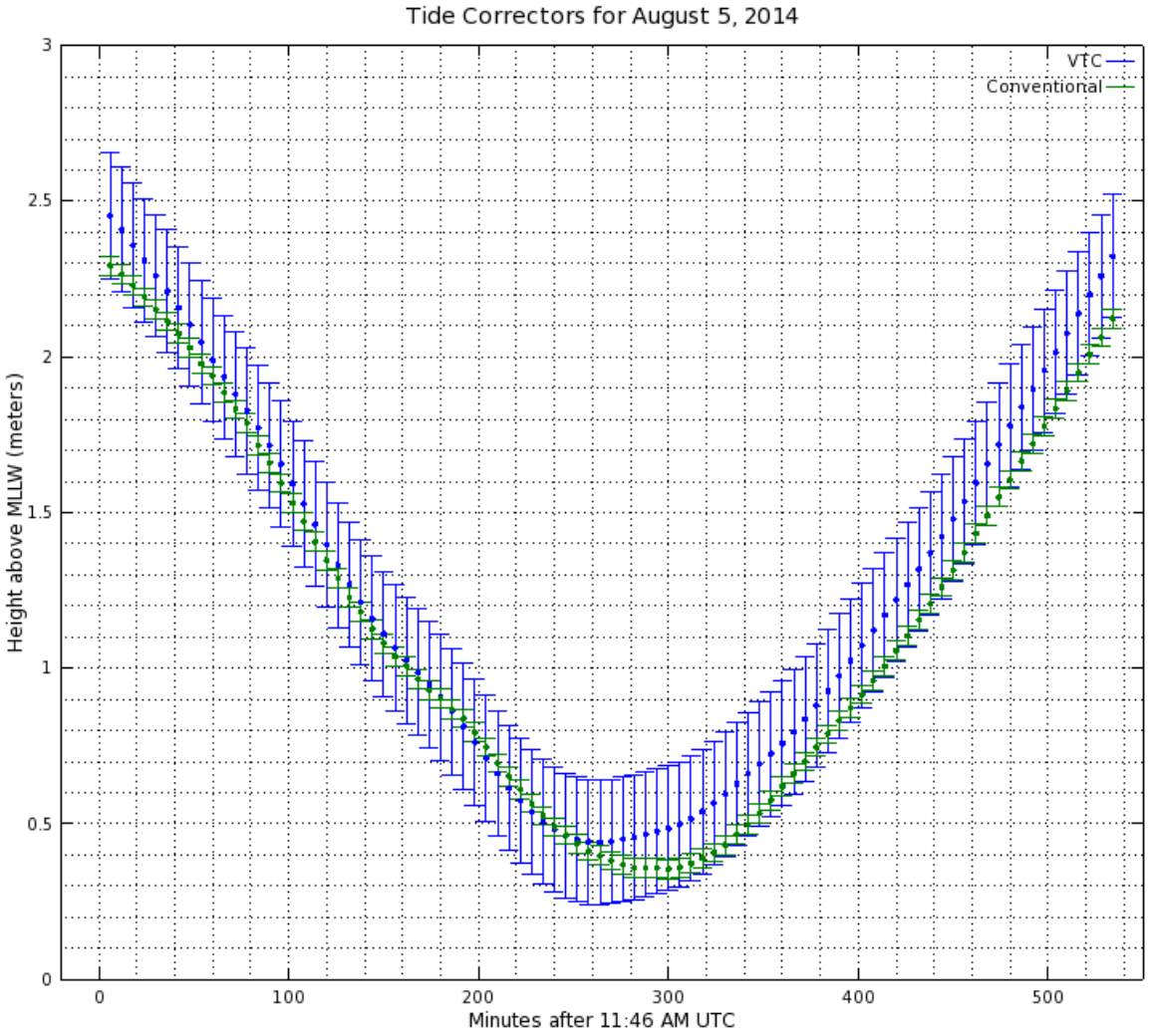

Figure 11– Tide Correctors for August 5, 2014.

For August 5, the data exhibited very good agreement during the ebb period after beginning with about 15 centimeters of difference. At approximately the 260th minute, the conventional data began an excursion with respect to the VTC data from which it did not fully recover. Even during the excursion, however, the conventional data never fell below the calculated uncertainty for the lower limit of the VTC data. From the 320th minute, the slope of both sets of correctors was nearly identical until the end of collection.

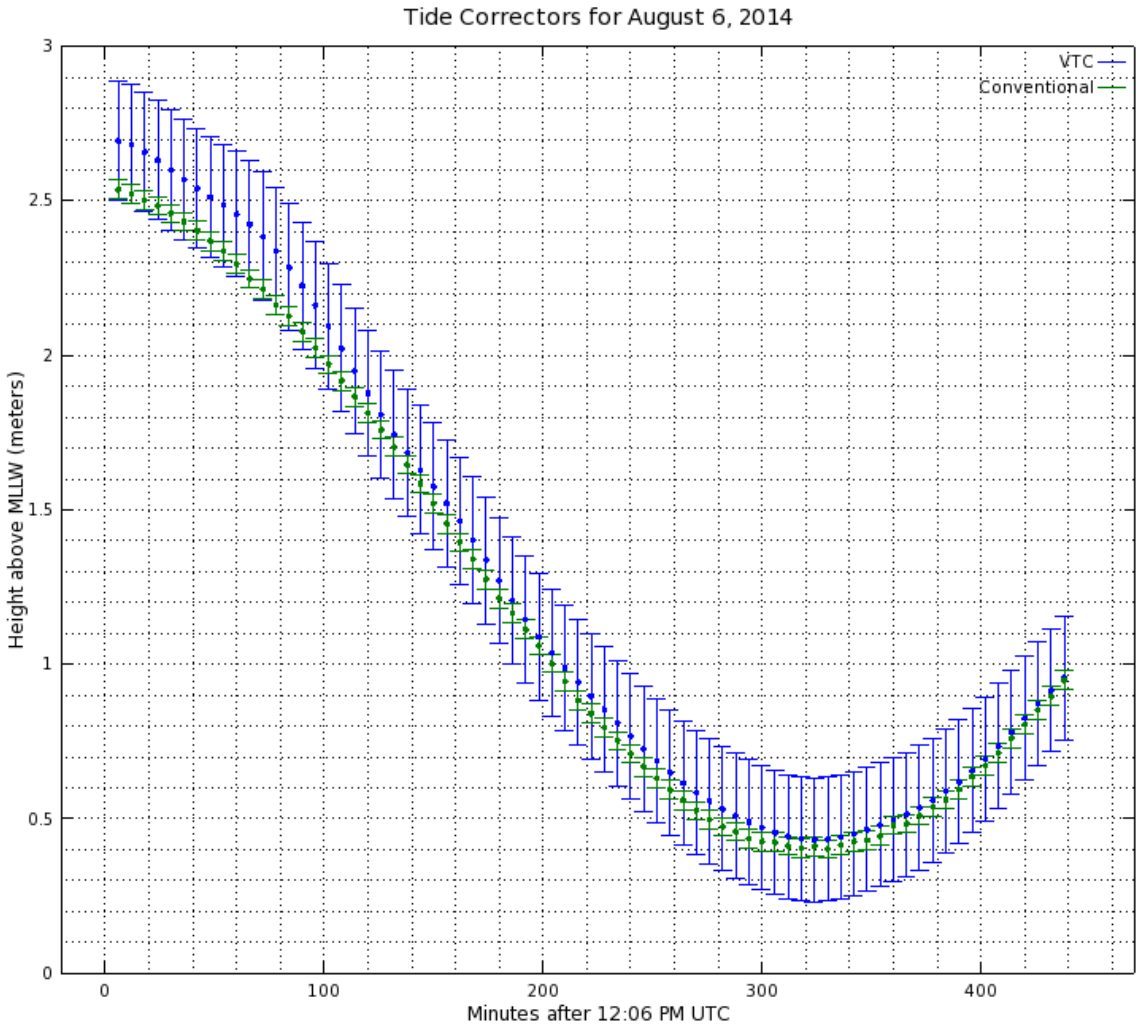

Figure 12 – Tide Correctors for August 6, 2014.

The data from August 6 showed very good agreement between the VTC and conventional data, especially from the middle of the ebb period through the end of collection. A 15-centimeter difference at the beginning of collection still placed the conventional data within the expected uncertainty of the VTC data. After the data began to agree very well at approximately the 120th minute, the difference between the two time series was considerably smaller than the lower limit of expected uncertainty.

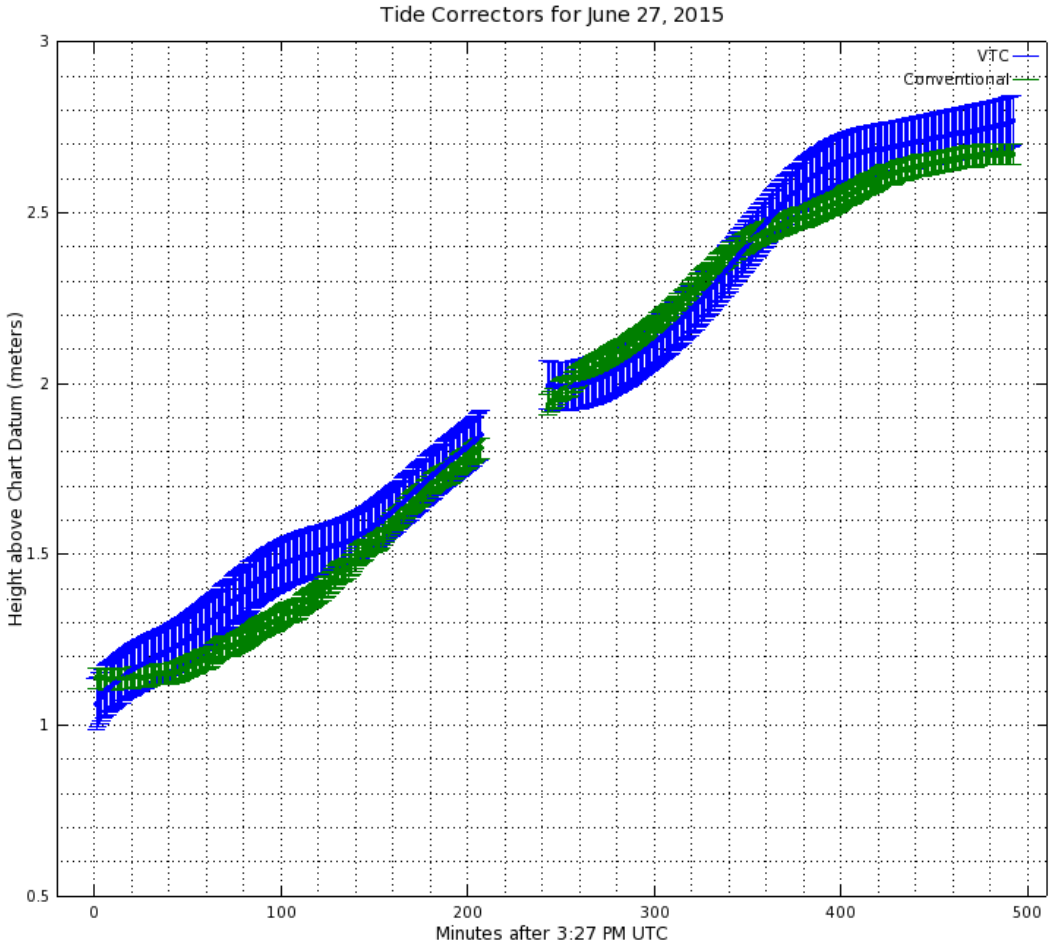

Figure 13 – Tide Correctors for June 27, 2015.

The first day of the second collection period was divided into two periods because HSL 16 went outside the target area for this experiment for a brief period. The data began with fairly good agreement, but a positive excursion by the VTC data left its expected uncertainty limit above the conventional data for approximately 80 minutes. At the end of the first 200 minutes, the difference decreased to less than a decimeter. From the beginning of the second division, the data agreed very well. All conventional data from that division were within the calculated VTC uncertainty. For almost two hours, the VTC data were lower than the conventional. For the final

50 minutes as high tide approached, the difference once again became positive, ending at approximately 10 centimeters.

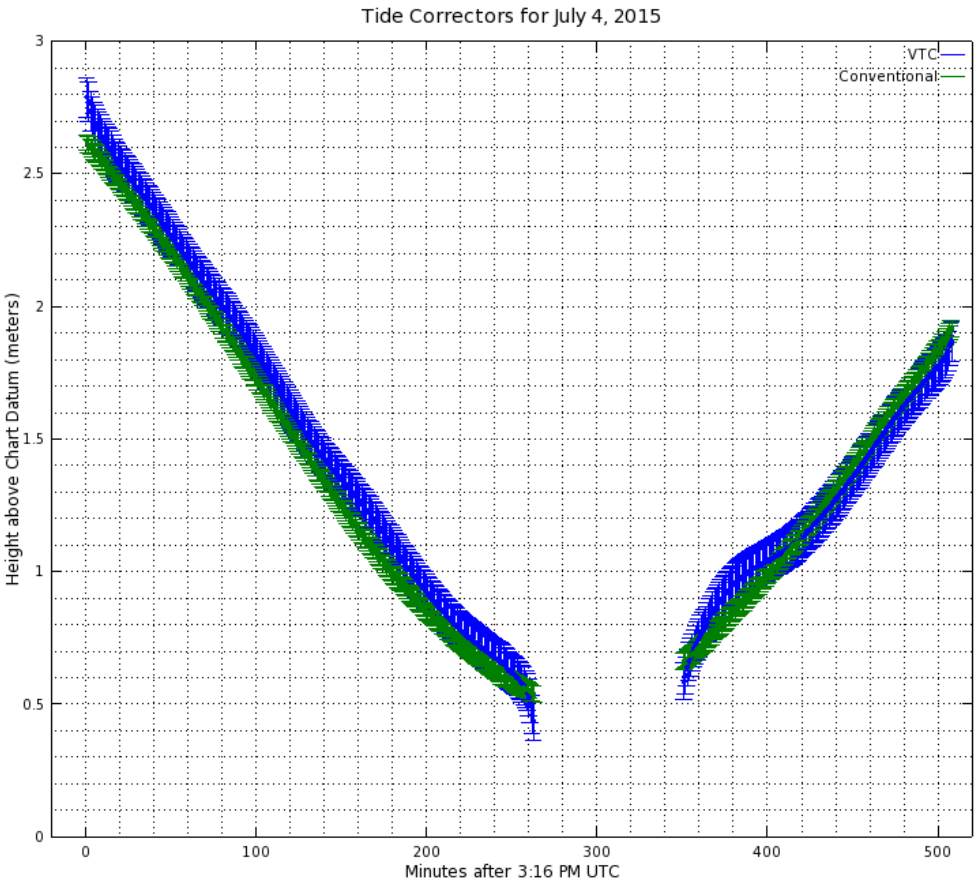

Figure 14 – Tide Correctors for July 4, 2015.

The second day of the second collection period was also divided into two periods because HSL 16 again went outside the target area. The first division is from an ebb period, and the second division is from a flood period, with low tide occurring outside of the data collection. During the ebb period, the VTC data were consistently higher than the conventional data, but the calculated lower limit of VTC uncertainty always encompassed the conventional correctors. The

flood period also showed fairly good agreement. The conventional data remained within the calculated VTC uncertainty through most of that period. There was an increase in the slope of the conventional data from the 60th to the 110th minute that was not captured in the VTC data, but the resulting height change was within the expected uncertainty.

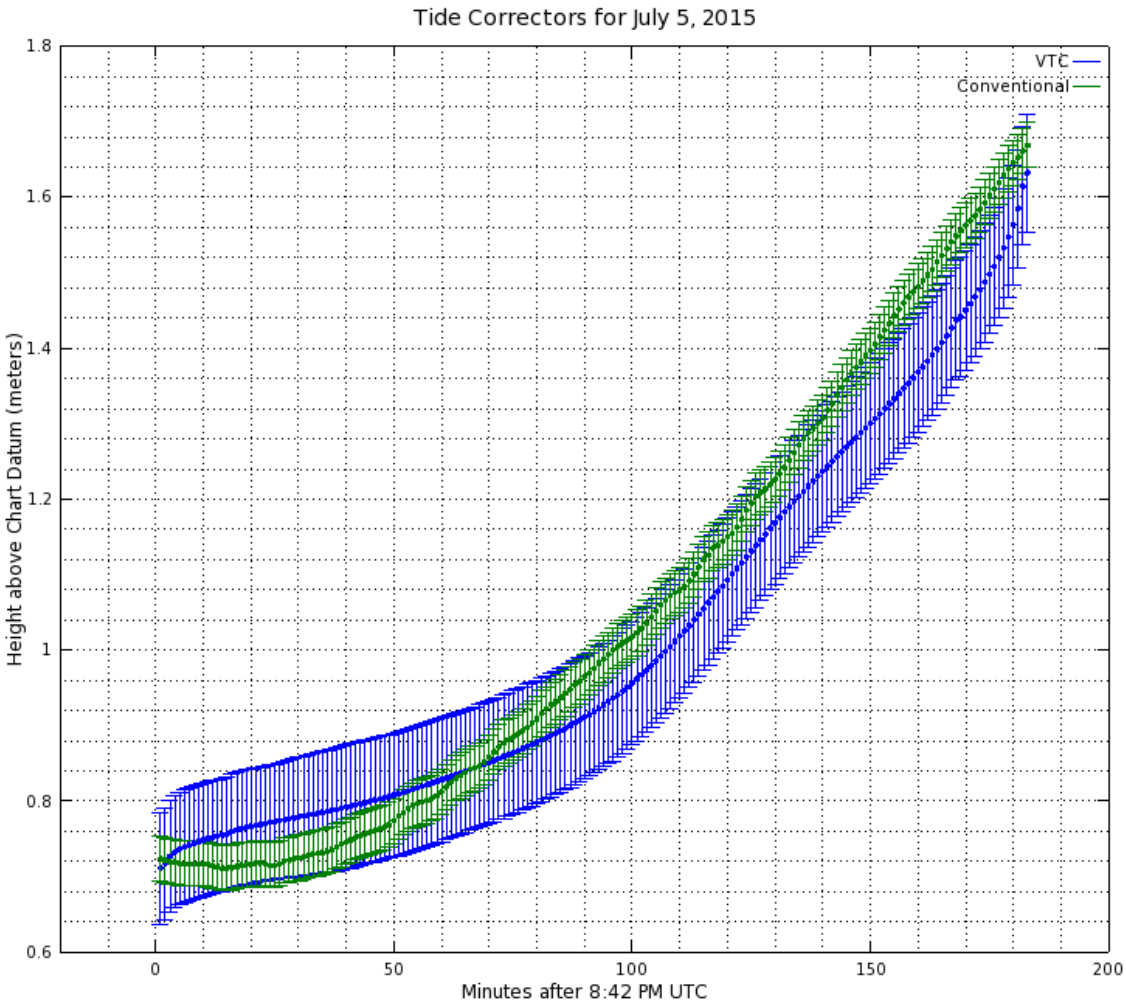

Figure 15 – Tide Correctors for July 5, 2015.

July 5th's data were exclusively from a flood period. The conventional data began with a downward inflection and followed with an upward turn, both of which were more drastic than what was found in the VTC. The upward turn resulted in the conventional data crossing over to

become larger than the VTC data at the 105th minute. The calculated uncertainty encompassed the conventional data until approximately the 140th minute. Near the end of the collection, the VTC value sharply increases and ends 8 centimeters below the conventional data.

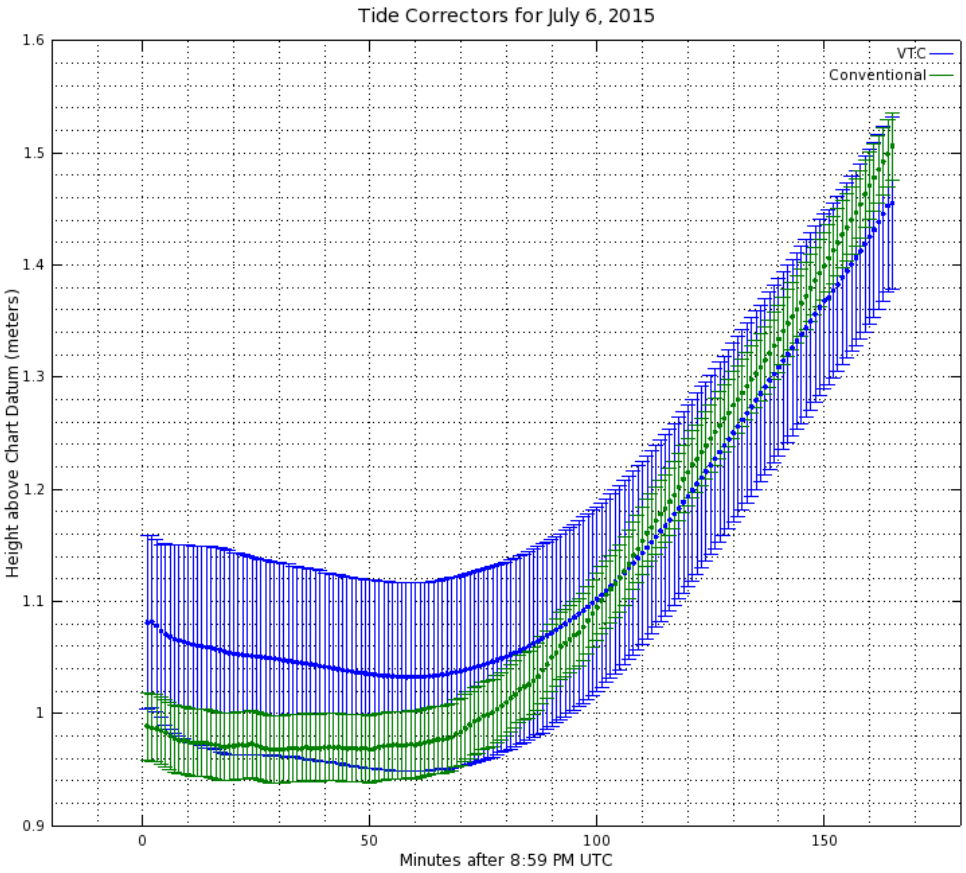

Figure 16 – Tide Correctors for July 6, 2015.

For July 6, the data were also in a flood period and exhibited similar characteristics to those data from the previous day. One notable exception is that the July 5 data began with good agreement and then diverted while the July 6 data began with a 10-centimeter difference. Before the 90th minute, the conventional data were either outside or on the lower edge of the calculated uncertainty limit. From the 90th to the 160th minute, the conventional data increase more sharply, going from the lower uncertainty limit to the upper one.

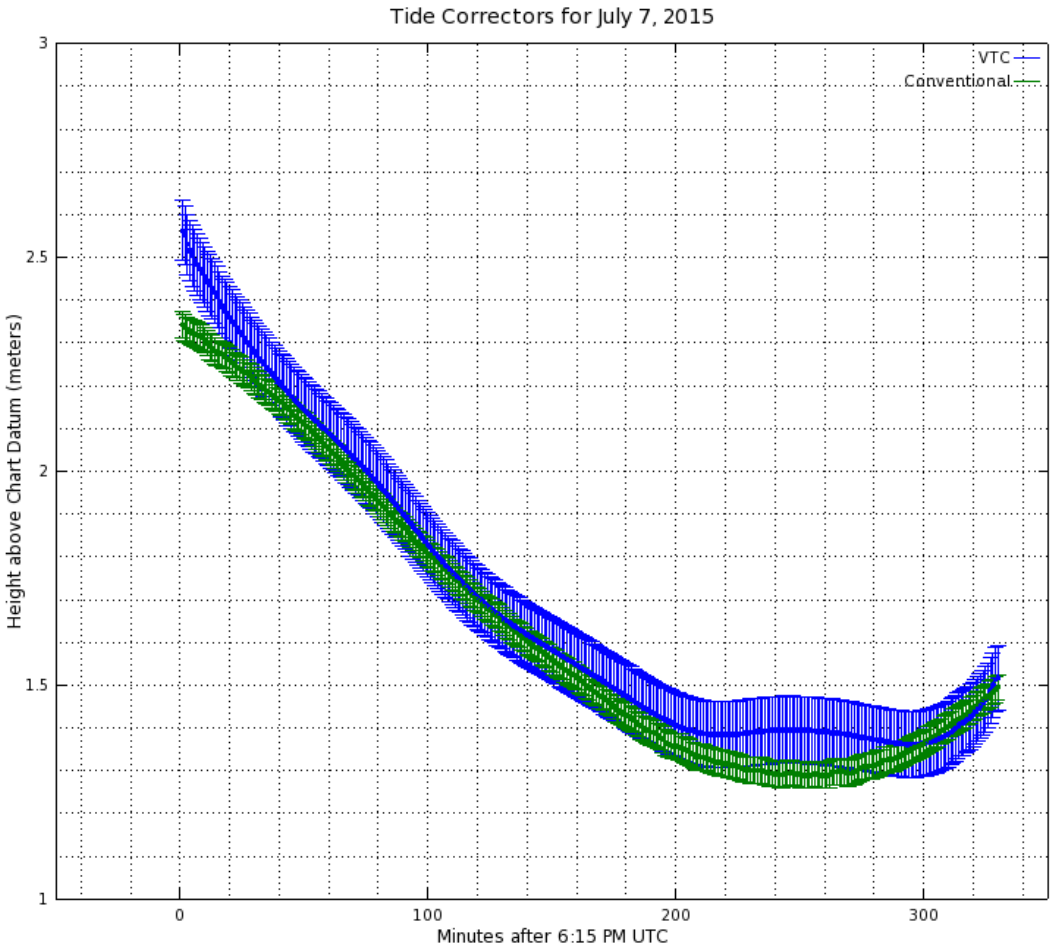

Figure 17 – Tide Correctors for July 7, 2015.

The data from July 7 moved from an ebb period to low tide. The difference began at approximately 20 centimeters, but it decreased over the first hour and remained in the lower uncertainty limit of the VTC until the 220th minute. The VTC data exhibited an upward inflection when the conventional data were at low tide, but the data began to agree considerably better 30 minutes before the end of collection.

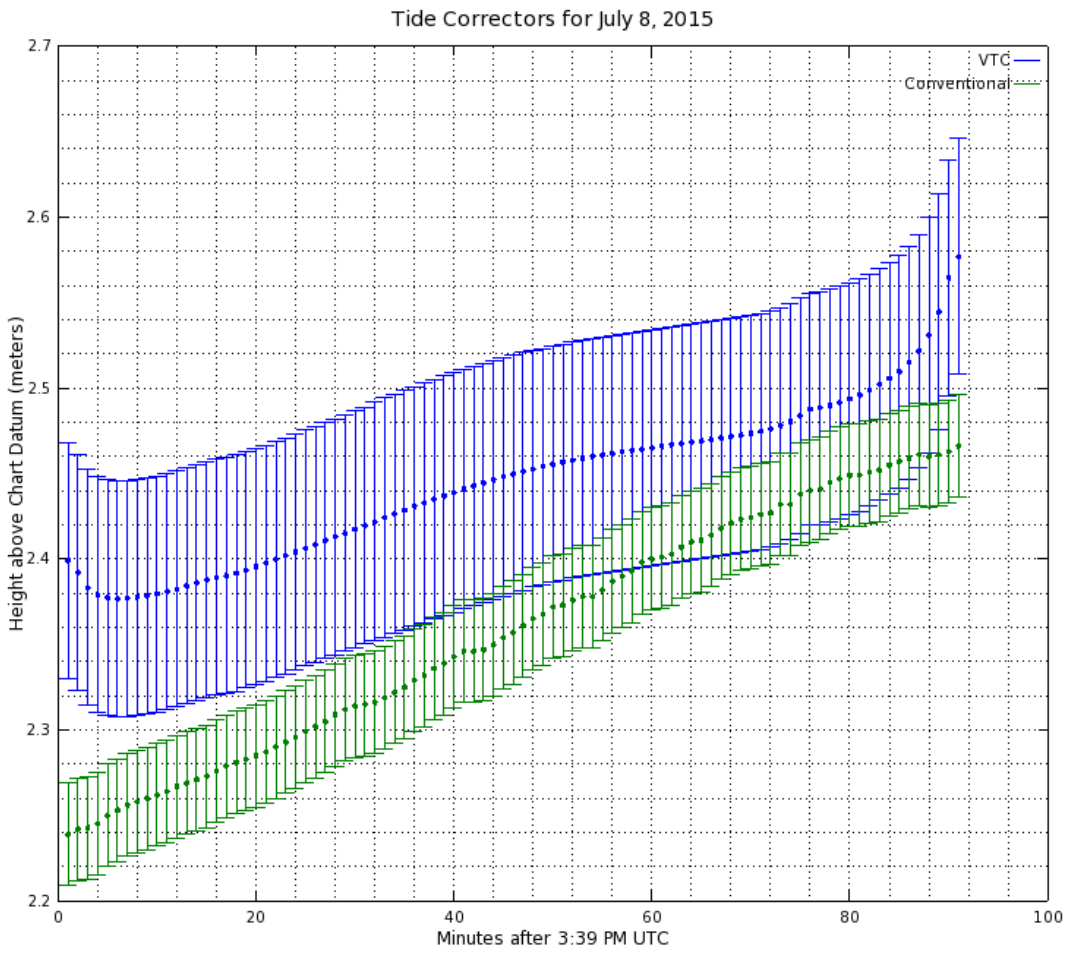

Figure 18 – Tide Correctors for July 8, 2015.

The final data collection occurred during a short flood period. The data began with a 16-centimeter positive difference. Through the collection, the conventional data increased more rapidly than the VTC. At the 59th minute, this increase cause the conventional data to come within the lower VTC uncertainty limit and remain there for 27 minutes. The VTC data show increases on both leading and trailing ends that are not present with the conventional data.

VII. Error Analysis

A. First Collection Period

The most significant element of the difference between VTCs and conventional correctors in the first collection period is the overall mean difference of approximately 8 centimeters. Although neglecting vessel motion expectedly contributed to the uncertainty of the VTC measurement, the preponderance of the virtual measurement suggests either a miscalculated vertical offset or an unaccounted effect of ship motion.

In view of the assumptions from Section V, Subsection A, it is evident that periods of small roll and large positive pitch would place the antenna higher above the waterline and result in larger antenna height measurements. Since the antenna to waterline correction was unchanged, larger antenna height measurements would result in a spuriously high VTC. The sea state for this collection period was calm for all three days, so it is reasonable to expect that the contribution of roll to the antenna's position may have remained relatively small. At the same time, the forward velocity of *Meriel B.* was observed to cause the bow to come up relative to the MRP, although the magnitude of this effect was not measured. Because the vessel was moving through most of the period, this cause is likely the largest contributor to spuriously high VTC.

Alternatively, vessel loading that caused it to ride higher in the water would have a similar effect on VTC measurements. Care was taken to measure the antenna height above the waterline while the loading best approximated what would occur during collection, but this factor remains a significant source of uncertainty.

Another significant element of the difference between VTCs and conventional correctors during the first collection period is the decreasing magnitude of the difference at low tide. The overall point in the tide cycle would be expected to have no appreciable effect on the

measurement of EH data or on the size of the SEP. It is possible that an effect of either the frequency space filtering or the smoothing is to modify the ends of the time series with respect to the middle. For instance, in the data from August 4, each end of the VTC time series is offset with respect to the conventional by almost 20 centimeters. At low tide, however, there is almost no difference between the two series. A change in the smoothing method might result in better performance near the boundaries. It is worth noting, however, that if this method were to be used operationally, the input data collected for it would be much more continuous than those data collected for this experiment and would result in significantly less data near the boundaries.

Typical VTC uncertainties for the first collection period were on the order of 20 centimeters at 1 standard deviation. This value corresponds to 39 centimeters at 2 standard deviations, and the IHO Order 1 allowable TVU for 50 meters of total water depth is 82 centimeters. (The depth of 50 meters is significant because it is often the shallow limit in which AUV multibeam data will be collected and thus is the most stringent case with respect to TVU.) Since almost 48% of the allowable TVU would be consumed by the tide corrector alone, it would be difficult to achieve even minimal IHO Order 1 vertical uncertainties in a hydrographic survey using this implementation of the technique.

B. Second Collection Period

This collection period features only one continuous dataset over 300 minutes in duration, placing significantly more data near a boundary, thus making it susceptible to the effects of improper smoothing. (Data from June 27 and July 4 each had discontinuities.) Those effects are apparent in the difference in the overall shapes of the curves as well as in more rapid undulations. In particular, three days (July 4 – 6) see the VTC data cross over the conventional data (i.e., go from greater than to less than) exactly once over the course of a flood period. This loss of definition in the shape of the curve suggests unintended performance not only near the boundaries but also in the center of each dataset. Further testing with longer duration datasets would be required to separate these two potential issues.

There was a lower overall mean difference compared to the first period, and this outcome is most likely attributed to precise measurement of vessel offsets and proper accounting of real-time attitude angles. Unlike the first period, the mean difference here is only a secondary issue and would likely remain well inside the expected uncertainty limits in the absence of unintended smoothing.

VTC uncertainties for the second collection period ranged from 7 to 9 centimeters with a mean of 7.4 at 1 standard deviation. This mean value corresponds to 14.5 centimeters at 2 standard deviations and represents less than 18% of the allowable TVU for IHO Order 1 for 50 meters of total water depth. It is clear that the addition of precise measurement of the antenna height above the waterline allows for a much lower overall uncertainty, thereby making possible the suitability of VTC data to provide vertical corrections in support of IHO Order 1 hydrographic AUV surveys.

VIII. Future Work

The results from these two collection periods demonstrate that the technique can offer an alternative source of water level information and can potentially do so accurately and precisely enough to support an AUV-based hydrographic survey. After examining these results, four issues persist that must be fully explored before this technique can be universally applied to shallow water AUV surveys.

First, any absolute difference between conventional and VTC measurements must be isolated and minimized. To accomplish this task, a particular vessel that would be used to collect EH data for the technique should remain very close (perhaps within 50 meters) to a shore-based gauge in an area with a well-defined SEP value. It should remain unmoored in that location for a duration of at least one day and up to several days. Application of this technique should yield results that are both well within the expected uncertainty and with a very small mean difference with respect to conventional measurements. Any other discrepancy here would indicate an error in offsets, motion, SEP calculation, or some other systematic error.

Second, the effects of smoothing on the shape of the VTC curve should be evaluated. During the unmoored test described above, the unfiltered (and untransformed) VTC data should be subjected to increasingly stringent filtering, beginning with almost no smoothing of the data. The point at which the smoothing begins to disturb the VTC data such that it loses the shape of the conventional data should be determined. The technique should then be modified to include enough smoothing to remove small noise but to stop short of the aforementioned point.

Third, any influences on antenna height above the waterline not yet accounted for should be thoroughly measured and should become a part of the technique. Particularly, the distance from an arbitrary point on the vessel to the waterline could be measured by a laser sensor as

suggested by Forbes et al. Having a direct, real-time waterline measurement would nearly eliminate s_{WLZ} as well as the problems of dynamic loading and squat effects.

Fourth, the distance over which the technique provides valid results should be tested. It will be useful to locate an area that contains a long (e.g., 10 nautical miles), straight line over which a well-defined SEP value has very little (< 5 centimeters) change. The surface vessel should move from the tide gauge (at one end of the long line) to the other side continuously over one day. VTC measurements should be separated into bins based on the surface vessel's distance from the conventional gauge. At some distance away from the gauge, the discrepancy between the VTC and the conventional measurements should exceed a threshold of desirability. If the most convenient area that meets those constraints is in the open ocean, the conventional tide gauge may have to be replaced with a GNSS buoy collocated with a bottom-mounted tide gauge.

IX. Conclusion

The importance of providing vertical correctors for AUV multibeam data and the fact that traditional shore-based gauges may not be available underscore the need for this VTC calculation technique. Additionally, this technique will allow for rapid in-field assessment of data both internally and with respect to data from surface platforms. When provided with precise inputs, it offers a favorable alternative to both the high uncertainty of predicted tidal correctors and the strict collection requirements of traditional tidal data. When the vessel collecting EH data lacks a motion sensor and thus requires estimation of the height of the GNSS antenna above the waterline, the uncertainty achieved by the technique is too large for the resultant VTC data to be used for hydrographic survey. If, however, the vessel attitude is an input to the system, uncertainty can be managed sufficiently to allow for those data to provide vertical corrections for AUV hydrographic data.

Precise measurement of all input parameters as well as proper mathematical manipulation of the VTC series must be achieved in order to minimize uncertainty. Modifications to this technique could result in a VTC series that more accurately represents the shape of the corresponding conventional tide curve, but the technique as it was described in this thesis is sufficient to provide vertical correction to IHO Order 1 AUV multibeam data. Future testing is required to isolate systematic inaccuracies, to refine the mathematical manipulation of the VTC data, to minimize input uncertainties, and to quantify the spatial limits of the method.

References

Bracewell, Ronald N. *The Fourier Transform and Its Applications*. 3rd ed. New York: McGraw-Hill Science/Engineering/Math, 1999. Print.

Brennan, Richard, Kurt Hess, Lloyd Huff, and Steve Gill. "The Design of an Uncertainty Model for the Tidal Constituent and Residual Interpolation (TCARI) Method for Tidal Correction of Bathymetric Data." Paper accepted for publication in the proceedings of U.S. Hydro 2005, March 29-31, 2005. San Diego, California. Web. February 10, 2015.

Byrne, Shannon, Walter Simmons, Gail Smith, and Bill Mehaffey. "A Demonstration of GPS Based Vertical Control, Unaided by a Shore Station." Presentation of Shallow Survey 2008, October 21-24, 2008, Portsmouth, New Hampshire. Web. February 10, 2015.

Diebel, James. "Representing Attitude: Euler Angles, Unit Quaternions, and Rotation Vectors." 2006. Stanford, California: Stanford University. Web. July 17, 2015.

Dodd, Dave, Jerry Mills, Dean Battilana, and Michael Gourley. "Hydrographic Surveying Using the Ellipsoid as the Vertical Reference Surface." *Facing the Challenges—Building the Capacity: Proceedings of FIG Congress 2010*. April 11-16, 2010, Sydney, Austrialia. Web. February 10, 2015.

Dodd, Dave and Jerry Mills. "Ellipsoidally Referenced Surveys (ERS); Issues and Solutions." Paper accepted for publication in the proceedings of U.S. Hydro 2011, April 25-28, 2011. Tampa, FL. Web. December 10, 2014.

Forbes, Steve, Phillip MacAulay, Chris Coolen, and Fred Carmichael. "A Laser-Based Water Level Sensor and Robust Insulated and Heated Multi-Well Stilling Well System for Ice-Prone Temperate and Sub-Arctic Environments." Presentation of U.S. Hydro 2009, May 11 – 14, 2009, Norfolk, Virginia. Web. April 8, 2015.

Gao, Yang. "GNSS Solutions: Precise Point Positioning and Its Challenges, Aided-GNSS and Signal Tracking." *InsideGNSS*, November/December 2006. Web. September 3, 2015.

Hiller, Thomas, Arnar Steingrimsson, and Robert Melvin. "Positioning Small AUVs for Deeper Water Surveys Using Inverted USBL." *Taking Care of the Sea: Proceedings of Hydro12*. November 12-15, 2012, Rotterdam, the Netherlands. Rotterdam: Hydrographic Society of Benelux, 2012. Print.

International Hydrographic Organization Special Publication No. 44. *IHO Standards for Hydrographic Surveys, 5th Ed*. International Hydrographic Bureau. Monaco, 2008. Web. February 13, 2015.

Ku, H. H. "Notes on the Use of Propagation of Error Formulas." *Journal of Research of the National Bureau of Standards—C. Engineering and Instrumentation*. 70C.4 (1966): (263-273). Web. August 14, 2015.

National Oceanic and Atmospheric Administration Special Publication NOS CO-OPS 1. *Tidal Datums and Their Applications.* Edited by Stephen K. Gill and John R. Schultz. February 2001. Web. August 11, 2015.

Press, William, Saul Teukolsky, William Vetterling, and Brian P. Flannery. *Numerical Recipes in C*. Cambridge, United Kingdom: Cambridge University Press, 1997. Print.

Rice, Glen and Jack Riley. "Measuring the Water Level Relative to the Ellipsoid During Hydrographic Survey." Paper accepted for publication in the proceedings of U.S. Hydro 2011, April 25-28, 2011. Tampa, FL. Web. July 5, 2015.

Riley, Jack and Bryan Murray. "GPS Water Level Buoy Uncertainty Case Study." Paper accepted for publication in the proceedings of U.S. Hydro 2015, March 16-19, 2011. National Harbor, MD. Web. July 4, 2015.

Weisstein, Eric W. "Nyquist Frequency." From MathWorld—A Wolfram Web Resource. http://mathworld.wolfram.com/RotationMatrix.html.

Weisstein, Eric W. "Rotation Matrix." From MathWorld—A Wolfram Web Resource. http://mathworld.wolfram.com/RotationMatrix.html.

Wert, Travis D. *Tidal Height Retrieval Using Globally Corrected GPS in the Amundsen Gulf Region of the Canadian Arctic*. MS thesis. The University of New Bruswick, Fredericton, Canada. 2004. Web. August 14, 2015.

Vita

The author was born in Picayune, Mississippi. After attending Picayune Memorial High School, he earned his bachelor of science in physics from The University of Alabama in 2008. He began his career with the Federal Government at Naval Oceanographic Office in 2009 where he currently investigates the problems of hydrographic survey and their solutions. He began his study of applied physics at The University of New Orleans in 2009.